Experimental and Numerical Investigation of Airflow and Contaminant Transport in an Airliner Cabin Mockup

Zhao Zhang, Xi Chen, Sagnik Mazumdar, Tengfei Zhang, and Qingyan Chen[*]

School of Mechanical Engineering, Purdue University, 585 Purdue Mall, West Lafayette, IN 47907, USA

Abstract

The study of airflow and contaminant transport in airliner cabins is very important for creating a comfortable and healthy environment. This paper shows the results of such a study by conducting experimental measurements and numerical simulations of airflow and contaminant transport in a section of half occupied, twin-aisle cabin mockup. The air velocity and air temperature were measured by ultrasonic and omni-directional anemometers. A gaseous contaminant was simulated by a tracer gas, sulfur hexafluoride or SF_6, and measured by a photo-acoustic multi-gas analyzer. A particulate contaminant was simulated by 0.7 µm Di-Ethyl-Hexyl-Sebacat (DEHS) particles and measured by an optical particle sizer. The numerical simulations used the Reynolds averaged Navier-Stokes equations based on the RNG k-ε model to solve the air velocity, air temperature, and gas contaminant concentration; and employed a Lagrangian method to model the particle transport. The numerical results quantitatively agreed with the experimental data while some remarkable differences exist in airflow distributions. Both the experimental measurements and computer simulations were not free from errors. A complete and accurate validation for a complicated cabin environment is challenging and difficult.

Keywords: airflow, transport and dispersion of aerosol contaminants, measurements, CFD, aircraft cabin

1. Introduction

More people including those having impaired health or who are otherwise potentially sensitive to cabin environmental conditions are traveling by air than ever before. The flying public would demand for a higher comfort level and a cleaner environment, because they encounter a combination of environmental factors including low humidity, low air pressure, and sometimes, exposure to air contaminants, such as ozone, carbon monoxide, various organic chemicals, and biological agents. Environmental Control Cystems (ECS) in airliners are responsible in delivering a comfortable and healthy cabin environment. In order to design a better ECS or improve how ECS operates, it is essential to study how the air and contaminants are transported and distributed in cabins.

The study can be achieved by either experimental measurements and/or computer modeling. Because the experimental measurements are expensive and slow, computer modeling is

---

[*] Corresponding author: Q. Chen, Phone +1-765-496-7562, FAX +1-765-494-0539, Email: yanchen@purdue.edu

increasingly popular. However, modeling of airflow and contaminant transport in a commercial airliner cabin is very challenging because of the high turbulence intensity, unstable flow, complex geometry, high occupant density, and high thermal loads. Olander and Westlin [1] used a zonal model to calculate airflow and concentrations in an aircraft cabin. The zonal model can only produce approximate results since it only considers the macroscopic flow between zones. More precise numerical modeling tools are necessary to calculate accurately airflow and contaminant transport mechanisms inside cabins.

With the recent advances in computer technology, the application of computational fluid dynamics (CFD) becomes very attractive in modeling airflow in aircraft cabins because it is inexpensive and flexible in changing thermo-fluid boundary conditions. Aboosaidi et al. [2] simulated the airflow patterns in aircraft cabins with empty seats by CFD. They validated their numerical simulations with flow information obtained by hot-wire anemometers, thermocouples, and smoke visualization. Their numerical results qualitatively agreed with the measurement data. Mizuno et al. [3] adopted similar methods in both the CFD and the experiments, while they conducted additional simulations and measurements on the contaminant dispersion. They achieved qualitative agreement between the computed results and measured data due to the limitations in the resolution of their measuring locations. Besides the limited experimental capability, these early investigations have been conducted only in unoccupied cabins. It is important to determine the influence of buoyancy from passengers and crew on the airflow pattern and contaminant transport in cabins.

Singh et al. [4] used heated cylinders to simulate passengers on the seats in an aircraft cabin and conducted CFD simulations in the cabin with and without the cylinders. They compared the numerical results from the two cases and concluded that the airflow pattern in the occupied cabin can be significantly different from that in the unoccupied one.

These early studies on airflow and contaminant transport in airliner cabins are meaningful. However, the airflow patterns in the cabins used for validating numerical results were often determined by smoke visualization that may not be sufficiently accurate. Therefore, researchers have tried to conduct more precise experimental measurements of air velocity fields with higher resolution and better equipment. The data is essential for validating CFD simulations. Garner et al. [5] measured the air velocity field using three-dimensional ultrasonic anemometers and used the experimental data to validate the CFD results in an empty Boeing 747 cabin. They measured the velocity vector field in multiple cross-sectional and longitudinal planes. With sufficient measurement resolution in the longitudinal direction, they were able to show that the airflow pattern was not two dimensional and the longitudinal variations were significant. Their measurement resolution in the cross-sectional planes was not very high to determine the detailed airflow pattern. In addition, the probes of the anemometers have relatively large span size so the measured velocity was the averaged value from a considerably large measurement volume. So the data may not be suitable for point-by-point comparison with the CFD results.

More recently, Lin et al. [6] applied a Particle Image Velocimetry (PIV) system to measure air velocity field in a generic empty cabin and used the data to validate the numerical results simulated by large eddy simulation (LES). The details of the airflow field and turbulence energy spectrum were analyzed. Their LES results reasonably agreed with the experimental data.

However, the airflow pattern in an isothermal empty cabin can be very different from a cabin fully loaded with passengers [4,7]. It is important to obtain quality experimental data in an occupied cabin or cabin mockup.

Mo et al. [8] used a PIV system to measure airflow in a section of a single-aisle occupied cabin with 18 passenger seats. Their study intended to generate high quality data for validating numerical results. They used a heated human-shaped manikin on one seat and 17 heaters on the other seats to simulate the actual thermal environment in a cabin. During the measurements, they lowered many seat-backs to clear the optical paths needed for the PIV system. So the geometric conditions they studied were not the same as those in reality although the overall thermal load well represented the actual conditions. Zhang et al. [7] also applied the Volumetric Particle Streak Velocimetry (VPSV) to measure the airflow patterns in a cabin in both emptied and occupied situations. In the occupied condition, the PIV measurement can only reach the upper part of the cabin as the seats and manikins significantly blocked the light for showing the airflow paths. Their measurements encountered the same problem as Mo et al. did.

Nevertheless, these studies have confirmed that the heat generated from passengers in a cabin can remarkably influence on the flow field but it is difficult to measure accurately the flow. Some of the experiment, such as the cases using ultrasonic anemometers, cannot measure detailed boundary conditions due to the large size of the probes. In addition, most of the studies did not consider particulate contaminant transport in a cabin. Many contaminants or biological agents, such as viruses, are particles and may be transported differently from that for gases. In order to generate reliable and high quality experimental data for validating computer models, it is essential to measure the airflow, temperature, and gas and particulate contaminant transport in a cabin with heated manikins. A CFD simulation is also necessary in order to examine the usefulness of the experimental measurements. These formed the objective to perform the research reported in this paper.
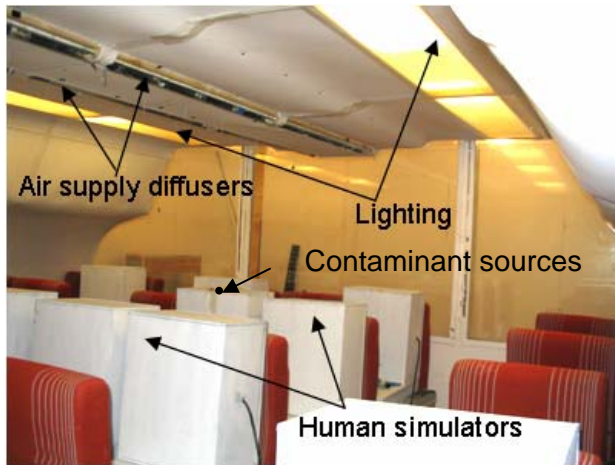
2. Experimental method

2.1. Experimental apparatus

Our experimental investigation to obtain reliable and high quality data was conducted in an environmental chamber and Figure 1 shows its outside view. A full sized twin-aisle aircraft cabin mockup was constructed inside the chamber. Figure 2 illustrates the interior view of the cabin mockup. The interior dimensions of the cabin at floor level were 4.9 m (X) $\times$ 4.32 m (Y). While the heights of the ceiling varied, the highest ceiling was 2.1 m from the floor. The cabin mockup had four rows with 28 passenger seats and 14 of them were with heated boxes (human simulators) that modeled seated passengers as shown in Figure 2. Light bulbs and mixing fans in the boxes generate uniform air temperature inside each human simulator. The total heat load for each human simulator was 83 W. Air was supplied at the ceiling level from two linear slot diffusers and exhausted from the outlets at the floor level on the side walls. A tracer gas, sulfur hexafluoride (SF_6), was used to simulate a gaseous contaminant. Non-evaporative, monodispersed Di-Ethyl-Hexyl-Sebacat (DEHS) particles were also generated to simulate a particulate contaminant. Both gaseous and particulate contaminants were released through tubes
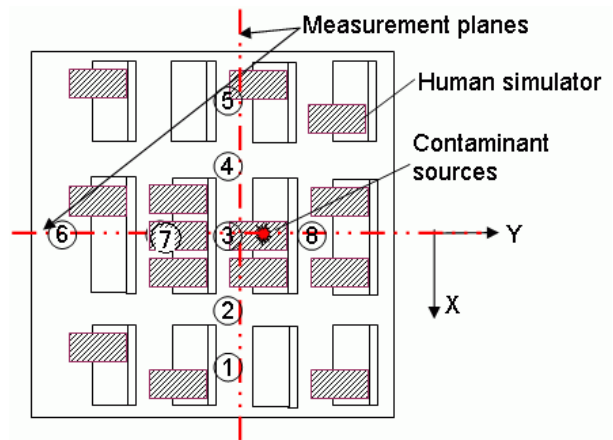
into the cabin on top of the middle passenger in the third row as shown in Figure 2. The experiment measured three-dimensional air velocity vector field and the distributions of air temperature, and the tracer gas and the monodispersed particles in the cabin.

Fig. 1. The outside view of the environmental chamber.

(a)   (b)

Fig. 2. The cabin mock up: a) field view of the mock up interior; b) top schematic view (circled numbers are positions for measuring contaminant concentrations).

The air velocity and temperature were measured by using two sets of Kaijo Ultrasonic Anemometer (DA-650) with TR-92T probes. The TR-92T anemometer probe had a 3 cm span size. The small span size minimizes the measurement error caused by volume averaging. The accuracy of the anemometers was 0.005 m/s with ±1% error for velocity components and 0.025 K with ±1% error for air temperature. In addition, the space in the occupied cabin was very limited, and only small sensors as such can fit into the gaps between human simulators and seats.

An INNOVA 1312 photo-acoustic multi-gas analyzer and an INNOVA 1309 multi-channel sampler were used to measure and sample the SF_6 concentrations. The monodispersed DEHS particles were generated by a particle generator (TSI 3475 CMAG). DEHS is a non-soluble liquid with a density of 912 kg/m^3 and a low evaporation rate. Since most particles stay in the room for a short time period, the size change due to evaporation was negligible. Under normal operation, the particle generator could generate monodispersed spherical particles with the geometric standard deviation (GSD) less than 1.2. In our experiment, the mean particle size generated was controlled to be 0.7 μm. This study used an optical particle sizer (TSI 3321 APS spectrometer) to measure the particle concentration and size distribution. To minimize the particle deposition on the sampling tubes, the experiment used a conductive silicone tube to deliver the particles to the source location and to sample the particles from different measuring locations in the cabin.

2.2. Experimental procedure

Before taking data, the environmental control system for the cabin was operated for around 48 hours to ensure a stable airflow and temperature distribution. The total airflow rate in the cabin was 0.23 m^3/s, corresponding to 25 air changes per hour (ACH) or 8.2 L/s per seat. The airflow rate was measured by using tracer-gas technique. An infrared thermometer was used to measure the surface temperature of the human simulators and the interior surfaces. We measured at least 10 positions on each surface. Although the surface temperature cannot be perfectly uniform, the averaged surface temperature well represented the thermal condition on each surface. Table 1 summarizes the averaged surface temperatures measured in this study, which are the input parameters for CFD simulations. Although accurate measurements of the boundary condition near the air supply inlet were very crucial for CFD simulations, the ultrasonic anemometers were not suitable. The linear diffusers had a width of only 2.5 cm, which was smaller than the sensor span size of the ultrasonic anemometer. This investigation used 16 omni-directional hot-sphere anemometers to obtain air velocity and temperature at five different heights near the diffuser as shown in Figure 3. The 16 hot-sphere anemometers were grouped and attached to a movable frame. The frame was adjustable both horizontally and vertically. A total of 560 points were measured along the two air supply diffusers on the cabin ceiling. Note that the omni-directional anemometers cannot measure air direction. The airflow direction at the diffusers was visualized by a smoke tester and the corresponding jet angles of air supply were recorded. The corresponding jet angles of air supply were estimated in both cross sectional and longitudinal directions. The detailed measurement data cannot be listed due to limited space in this paper. Although such a measurement could lead to significant errors, it was practical to quantify the jet behaviors coming out the linear air supply diffuser. Unless a laser Doppler anemometer (LDA) was used, it would be very difficult to determine the exact flow conditions from the diffusers. However, it would take months to complete such a measurement with an LDA.

Table 1. Measured temperatures in the cabin mockup.

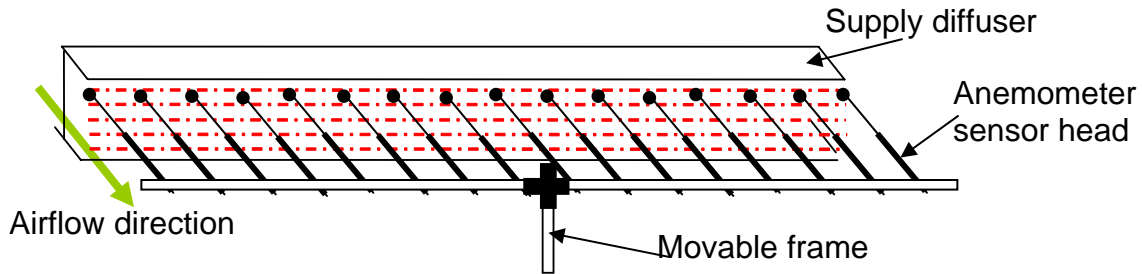| Supply air	19.3 ^{o}C	Floor along the aisles	24. 8 ^{o}C
Ceiling between diffusers	23.8 ^{o}C	Floor under central seats	25.1 ^{o}C
Ceiling between inlets and lighting	26.4 ^{o}C	Front / back wall	24.7 ^{o}C
Sidewalls	24.5 ^{o}C	Manikins	31 ^{o}C
Floor under side seats	24.4 ^{o}C	Seats	adiabatic

Fig. 3. The schematic arrangement of hot-sphere anemometers for measuring the velocity and temperature conditions at the air supply diffusers.

The experiment measured the air velocity and temperature inside the cabin with the ultrasonic anemometers. Since only two anemometers were available, they were moved manually from one location to another in the cabin in order to measure the air velocity and temperature fields. At each location, the anemometer measured the air velocity and temperature for at least four minutes at a measuring frequency of 20 Hz (about 4800 readings). The experiment also measured air velocity at several locations for longer period (around 20 minutes). The velocity statistics from the two measuring periods at the same location show no significant difference. Thus, four minutes of sampling time were sufficiently long. When an anemometer was moved from one location to another, the system was stabilized for about 10 minutes so to avoid recording the disturbance caused by moving the sensor. Since the air exchange rate in the cabin was very high, a 10-minute waiting time was sufficiently long to minimize the impact due to the movement. As shown in Figure 2(b), this investigation measured air velocity field in both the cross-sectional and longitudinal planes for a total of 103 locations. The air velocity experiment was repeated by two groups of researchers at different time to check the repeatability. The two sets of results were almost identical.

The tracer gas measurements started with monitoring SF_6 concentration at the air supply inlet and exhaust while the tracer gas was continuously released into the cabin with a volume flow rate of 5×10^{-8} m^3/s. The concentration became stable within 30 minutes. After reaching the steady state, the experiment then measured the tracer-gas concentration inside the cabin in eight locations as shown in Figure 2(b) at six different heights. The measurement in each location took about 30 seconds to sample the air. For each location, ten measurements were repeated. The

calculated standard deviation was less than 10% of the mean value at most locations except those close to the tracer-gas source with the highest standard deviation of 30% of the mean value.

The procedure of the particle concentration measurements was similar to that of the tracer gas. The particle concentration in the exhaust duct work was also monitored until it reached steady state, after the particles were injected to the cabin. The sampling probe was placed parallel to the mean flow direction in the exhaust duct, and the probe size ensured isokinetic sampling. The particle concentration in the duct work was about 4.4×10^8 (particles/m^3) in steady state. The particle concentration was measured at 50 positions in the two planes. Three to six samples were recorded at each position in order to analyze the concentration fluctuations. Each measurement continued for 60 seconds. The standard deviation of measurements was generally less than 15 percents of the mean value except one position closest to the particle source. Due to the highly fluctuated nature of both the flow and particle concentration near the source, ten consecutive measurements at this location were performed. The standard deviation of the measurement was about 25% of the mean value.

The particle deposition rate is of great concern in the cabin mockup. In principle, the deposition rate can be estimated by the differential between particle generation rate and exhaust rate assuming other particle dynamics (e.g., infiltration and resuspension) are negligible. This study first measured the particle concentration at the exhaust as stated above, and calculated the exhaust rate according the total airflow rate. For particles of 0.7 μm used in our study, the mean particle exhaust rate was close to the mean generation rate with a relative difference of 3%. Because our measurements had a standard deviation of about 10% of its mean value, the difference was much smaller than the deviation so it was impossible to estimate the deposition rate with the equipment and the current experimental setup. Nevertheless, the number well indicates that the deposition for such 0.7 μm particles seems insignificant compared with the particles removed by the environmental control system. For much finer or coarser particles whose deposition becomes significant, the current experimental method can be of insufficient accuracy. This limited our experiments for a wider range in particle size.

3. Numerical method

This study adopted Reynolds-averaged Navier-Stokes (RANS) equations with the renormalization group k-ε (RNG k-ε) turbulence model [9] to predict the distributions of airflow, temperature and tracer-gas contaminant. The model was selected because it has been successfully used to simulate airflow and contaminant transport in various enclosed environment [10-11]. The corresponding governing transport equations for the RNG k-ε turbulence model can be generalized as:

$$\frac{\partial(\rho\Phi)}{\partial t} + \mathrm{div}\left(\rho\vec{u}\Phi - \Gamma_{\Phi,\mathrm{eff}}\,\mathrm{grad}\left(\Phi\right)\right) = S_{\Phi} \tag{1}$$

where Φ represents the time averaged velocity components $\overline{u}_i$ (i=1,2,3), turbulent kinetic energy k, dissipation rate of turbulent kinetic energy ε, enthalpy H, and SF$_6$ concentration. When Φ is

unity, the equation represents the conservation of mass. Note that ū is the Reynolds-averaged air velocity vector, and t is time. Details about the terms and coefficients for different variables can be found in the CFD software documents [12] and are not repeated here due to limited space for the paper.

The study applied a Lagrangian method to predict particle dispersion and adopted the particle source in cell (PSI-C) model to calculate particle concentration distribution. The Lagrangian method calculates the motion of discrete particles in the air based on Newton's second law. The discrete random walk method was used to account for the turbulent dispersion of discrete particles. The PSI-C method could successfully convert the particle trajectories into a stable concentration field if significant number of particles was tracked and analyzed. The stability and the viability of the integrated Lagrangian method and the PSI-C model have been stated and validated by Zhang and Chen [13].

All the numerical simulations in this study were conducted using commercial CFD software, FLUENT (version 6.2). The computational mesh of the cabin contained 2.8 million tetrahedral cells. The study used the second-order upwind scheme for all the variables except pressure for the RANS equations. The discretization of pressure was based on a staggered scheme, PRESTO! [12]. The SIMPLE algorithm was employed to couple the pressure and momentum equations. The Boussinesq assumption was used to account for the buoyancy effect. In addition, ad hoc models for calculating the particle concentration distribution based on Lagrangian trajectories were implemented into FLUENT via user-defined functions. With the aid of the ad hoc models, the study could calculate the particle concentration simultaneously with the Lagrangian particle tracking in CFD. This facilitated concentration computation and made tracking millions of particles computationally affordable on a personal computer.

4. Results and analyses

4.1. Airflow and temperature field

The CFD simulations used the measured boundary conditions and the numerical method stated in the previous section. The CFD results were then compared with the experimental data.

Figure 4 shows the airflow patterns in two measured planes, a cross-sectional plane through the third-row seats and the center plane along the longitudinal direction. In the cross section, the airflow is not symmetrical. This is partly because of the asymmetrical air supply velocity profile and also the asymmetrical distribution of heated human simulators. The cross sectional view shows two large circulations in the cabin. The predicted flow paths (green lines) qualitatively agreed with the experimental data. However, remarkable errors exist in quantitatively comparison. For example, the CFD predicted strong downward air movement in the left cabin that did not show in the measurements. The CFD also calculated strong airflow in the region near the right ceiling, which was not captured by the field measurement. Those errors likely came from the flow boundary conditions from the jet diffusers. Although we measured the velocity magnitude at many points along the jets, the estimation of velocity direction by flow visualization may not be accurate because the airflow along the diffuser was highly non-uniform.

The results suggested the numerical simulation is very sensitive to the accuracy of boundary conditions.
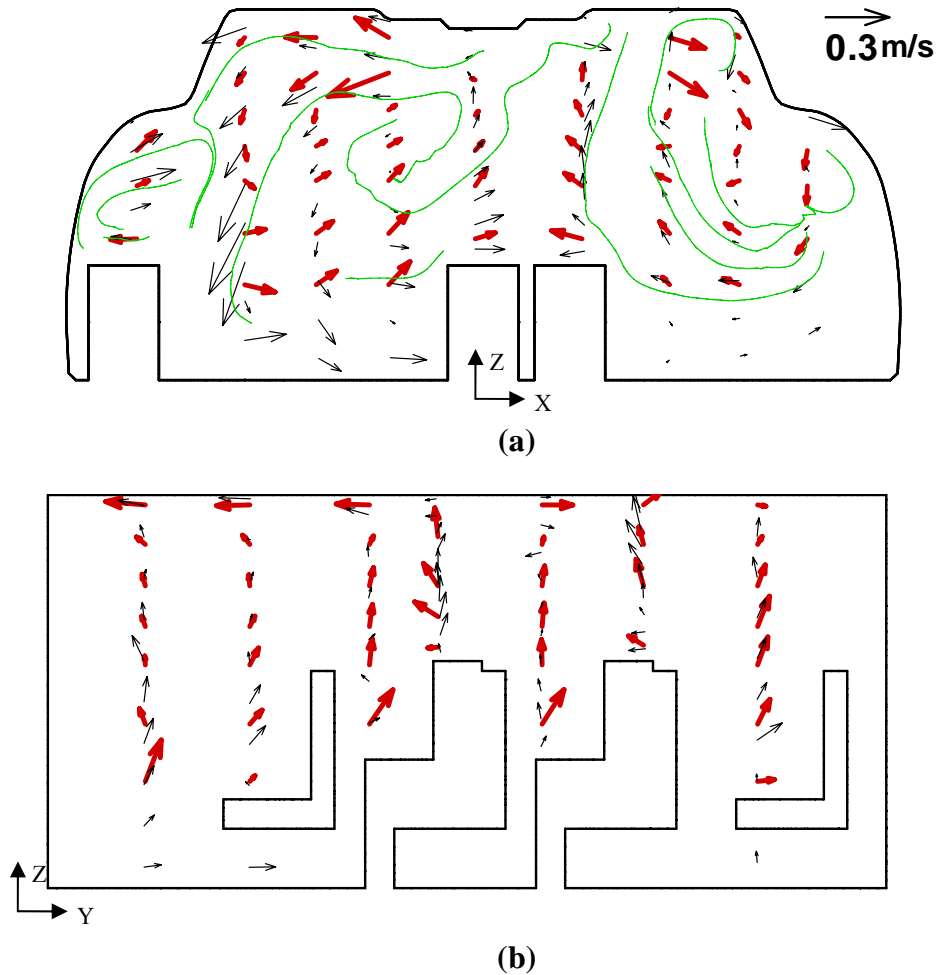

(a)

(b)

Fig. 4. Comparison of the airflow pattern measured (bold vectors in red color) and computed (light vectors in black color): (a) in the cross section (the green lines are flow paths computed); (b) in the mid-section along the longitudinal direction.

The numerical results agreed reasonably well with the experimental data on the longitudinal plane shown in Figure 4(b). Generally, the airflow in the center plane is unidirectional and upward due to the co-effect of two large circulations in cross sections and the buoyancy plumes from the passengers. The air moved forward near the ceiling in the two front rows and moved backward in the two back rows. The CFD can capture those main flow features in the center plane although some discrepancies still exist. For example, the predicted thermal plume from the passenger at the third row was not as strong as the measured one. This is probably due to the uniform surface temperature for human simulators used in CFD simulation, while uniform surface temperature was hard to be obtained in the experiment, although mixing was used in the human simulators.

Figure 5 shows the vertical temperature distribution profiles. The calculated temperature profiles agreed reasonably well with the measured data. The agreement for the air temperature is better than that for the air velocity. This is due to the strong mixing of air in the cross sections that created a very uniform temperature distribution in the cabin. Since both the experiment and the simulation were close to well-mixed conditions, it is not a surprise to see such good agreement in the air temperature distributions.

Fig. 5. Comparison of the measured (red symbols) and predicted (black lines) air temperature profiles in different locations in the cabin mockup (z is height from the cabin floor and $T = (T_{local}-T_{in})/(T_{out}-T_{in})$).

4.2. Contaminant dispersion and distribution

Figure 6 shows the tracer gas (SF_6) concentration profiles in various measured locations. The simulated tracer gas concentration does not agree with the measured data as that for the air temperature. Unlike the heat transfer occurred in the cabin that was with many heat sources, there was only one SF_6 source in the cabin. The mixing with a single source is more difficult than with multiple sources. Thus, the predicted SF_6 concentration distribution was less uniform compared with the temperature distribution, especially near the contaminant source. Position 3 was close to the SF_6 source. The SF_6 concentration in this region was highly non-uniform. Although the CFD predicted correctly the peak location in position 3, it over-predicted the magnitude. However, it is difficult to say if the measured value is more accurate. The unstable

10

airflow near the source could cause high concentration fluctuation and could contribute to the error. Yuan et al. [14] found similar problems in an office with displacement ventilation when the contaminant source was close to a heated mannequin.
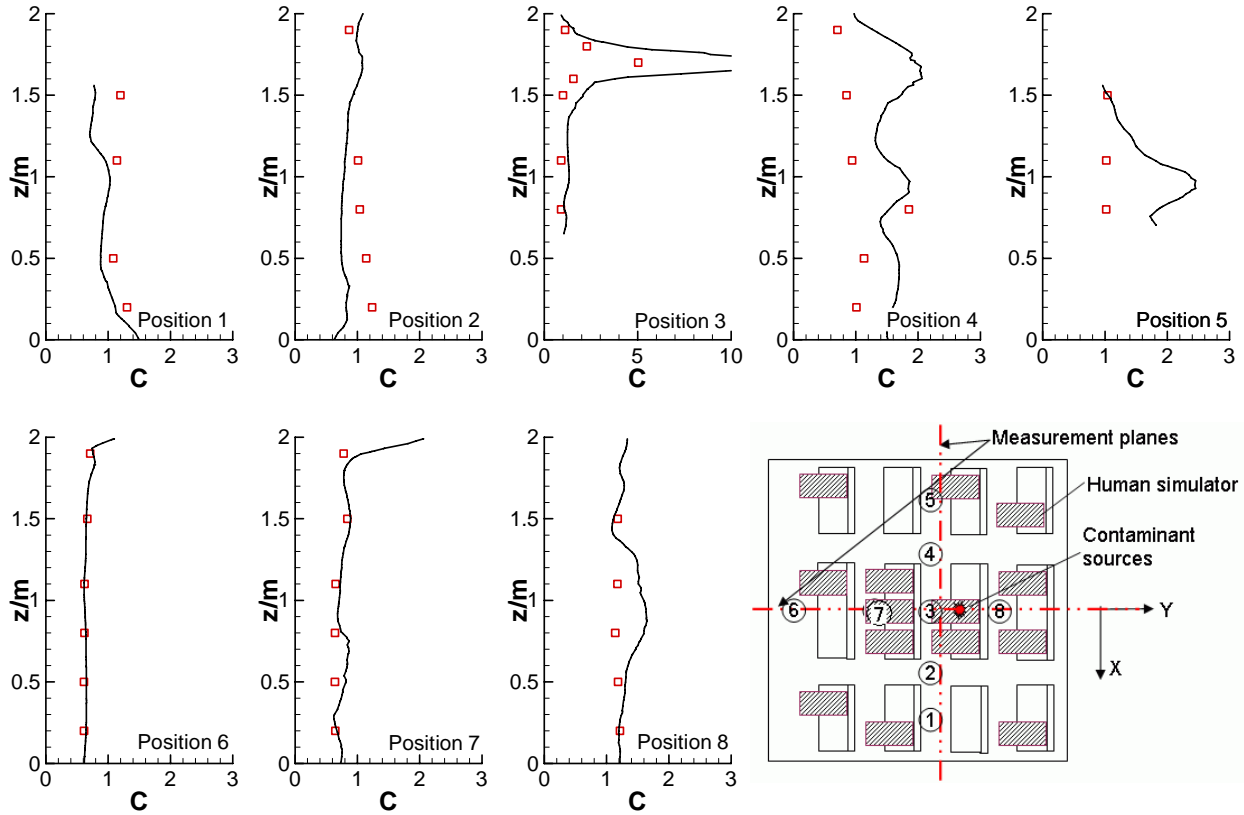

Fig. 6. Comparison of the measured (red symbols) and predicted (black lines) tracer gas concentration in different locations in the cabin mockup (z is height from the cabin floor and $C = (C_{local}-C_{in})/(C_{out}-C_{in})$).

The CFD also over predicted the SF_6 concentration at positions 4 and 5. This is probably caused by the discrepancies in the predicted and measured velocity fields. The predicted air circulation on the -X (starboard) side of the cabin mockup was stronger and entrained more SF_6 to the region. This led to a higher contaminant concentration compared with that on the port (+X) side of the cabin. On the other hand, the CFD results are reasonably accurate in regions far from the source such as positions 6, 7, and 8 in the longitudinal direction. When the SF_6 concentration became uniform and close to the average concentration, the concentration prediction became less dependent on the velocity field and agreed better with the measured data.

The modeling of particle transport in the cabin mockup is similar to that of the tracer gas, while additional assumptions were used for particle simulations. The particle concentration at the inlet was assumed to be negligible since it was two orders smaller than the mean concentration in the cabin. The study further assumed that the particle deposition was negligible compared with that

11

removed by the environmental control system, because a rough estimation of the deposition is about 10 percent of the nominal mean concentration. The particles in the Lagrangian simulation were assumed to be solid spherical particles with a uniform size of 0.7 μm in diameter. The density of the particle was 912 kg/m^3 , which was identical to the experimental DEHS particles. This study tracked and analyzed 500,000 particle trajectories to generate a reliable concentration distribution with sufficient stability.

Figure 7 compares the computed profiles of particle concentration with the experimental data. The peak concentration at the center line, position 3, was well predicted. However, the discrepancies are significant between the computed profiles at positions 1 and 2 and the data. Again, this is probably attributed to the difference between the simulated and measured airflow fields. The predicted air circulation on the starboard (-X) side entrained more particles and led to a higher particle concentration at the top part of position 4 and lower particle concentration at positions 1 and 2. Further, a significant portion of the tracked particles followed the strong downward airflow on the left half as shown in Figure 3(a) and left quickly from the exhaust. These particles lingered shortly in the cabin so not many were dispersed in the longitudinal direction. It seems that the Lagrangian method tended to over-predict the particle concentration decay in the longitudinal direction so low concentration was found at positions 6 and 7.
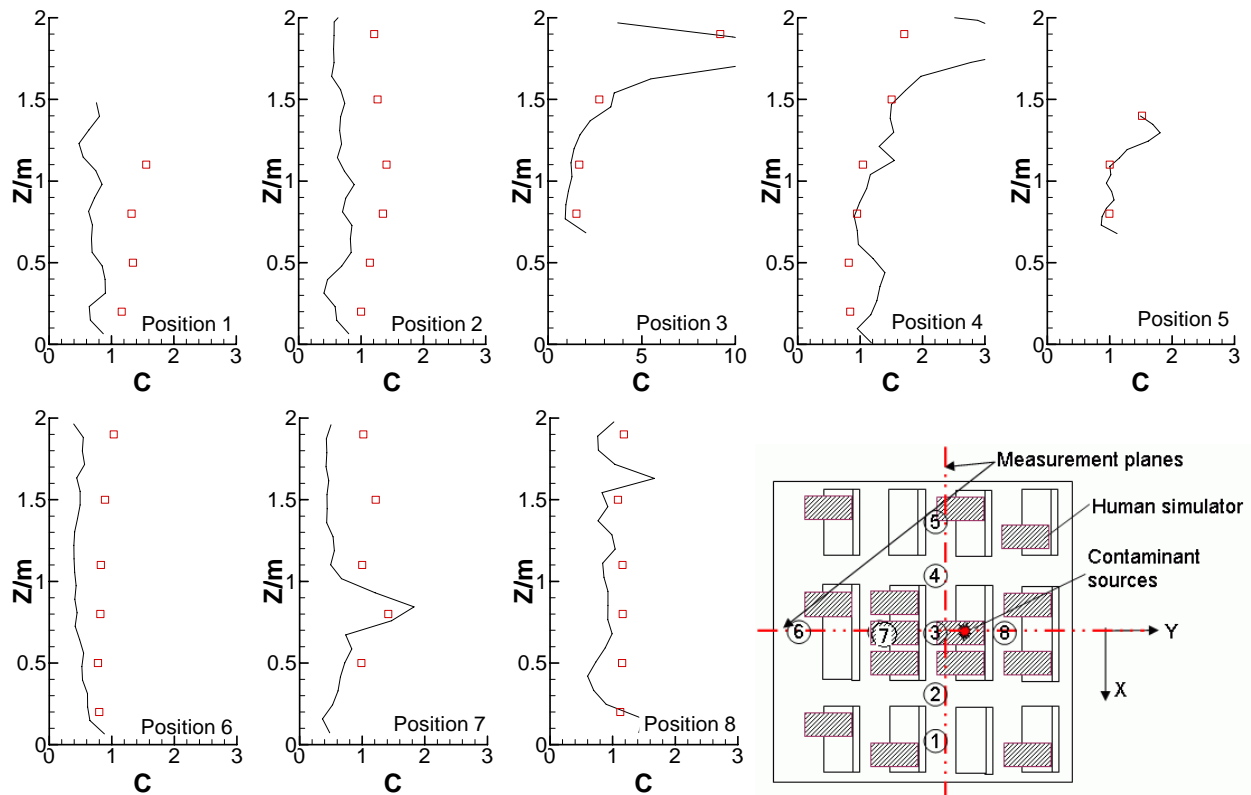

Fig. 7. Comparison of the measured (red symbols) and predicted (black lines) particle concentration distribution in different locations (z is height from the cabin floor and C = C$_{local}$/C$_{out}$).

5. Discussion

While this investigation has analyzed the errors between measured and simulated results for each physical quantity, it is also interesting to understand the similarities and differences of the transport and dispersion of different physical quantities. The performance of the CFD models seems depending on the quantities calculated. The calculated temperature distribution agreed very well with the experimental data although remarkable differences between measured and predicted velocity field existed. The predicted temperature distribution is not sensitive to the flow field because the general airflow pattern was close to well-mixed condition and the heat sources were uniformly distributed. On the contrary, accurate airflow prediction is very important in determining the contaminant transport. With only one point source for each contaminant, the concentration distribution near the single source was highly non-uniform. The mean airflow pattern and turbulence determined where and how the contaminants were transported and dispersed in the cabin. Therefore, the predicted tracer gas and particle concentrations have similar accuracy when compared with measured data.

It should be noted that transport and dispersion of gaseous contaminants may be different from those of particulate ones. In this study, the SF_6 and DEHS particles were released at the same location. Their normalized concentration distributions shown in Figure 8 illustrates that the distributions of the two contaminants were similar in most part of the cabin. This indicates that small particles behave like a passive tracer gas. This also implies that both the Eulerian and Lagrangian methods should have similar accuracy in predicting transport and dispersion of small particles as shown in Figures 6-8 as already being found by others [15-17]. However, the particle concentration was much higher than that of the tracer gas at the locations near the ceiling region in position 3. Since we collected sufficient data to derive the time-averaged concentrations, the measured difference was not merely due to the instable flow near the source. The turbulent dispersion of particles was slower than that of the tracer gas near the source so that the particles accumulated more in that region. Hence, the dispersion characteristics of micron-sized particles can still be different from that of a gas despite of their general similarity in the present study.

Figure 8 also shows that the contaminant concentration in the four-row cabin is rather uniform. This is not only because of the well-mixing airflow pattern but also due to the end-wall blockage in the longitudinal direction. The concentration should show a clearly decay in the traverse direction in a longer cabin [18]. It is thus necessary to further investigate the flow and contaminant transport behaviors in a longer cabin. At present, we are validating our model performance in a cabin model with sufficient longitudinal length to capture more contaminant transport characteristics in a real flight. A detailed presentation and discussion on this further investigation will be reported in the near future.

Baker et al. [19] investigated the airflow in an unoccupied cabin and found that the airflow was unsteady although the boundary condition was steady. This may raise the question whether the time averaged numerical simulations and experimental measurements used in this investigation are sufficient to depict the flow and contaminant transport in the cabin mockup. Our experiment and simulations found that the airflow was relatively stable in an occupied cabin. Although the thermal plumes from passengers generated fluctuations in the flow field, they also help break

down the most energetic and unstable large eddies. Therefore, the airflow and contaminant concentration was stable in most of cabin except in areas near the jets and contaminant sources. Zhang et al. [7] conducted a parametric study of velocity fluctuation levels with different occupancy rates. Their study also confirmed that the airflow in an occupied cabin was much more stable than that in an unoccupied one. Therefore, the time averaging method used in this investigation seems appropriate.
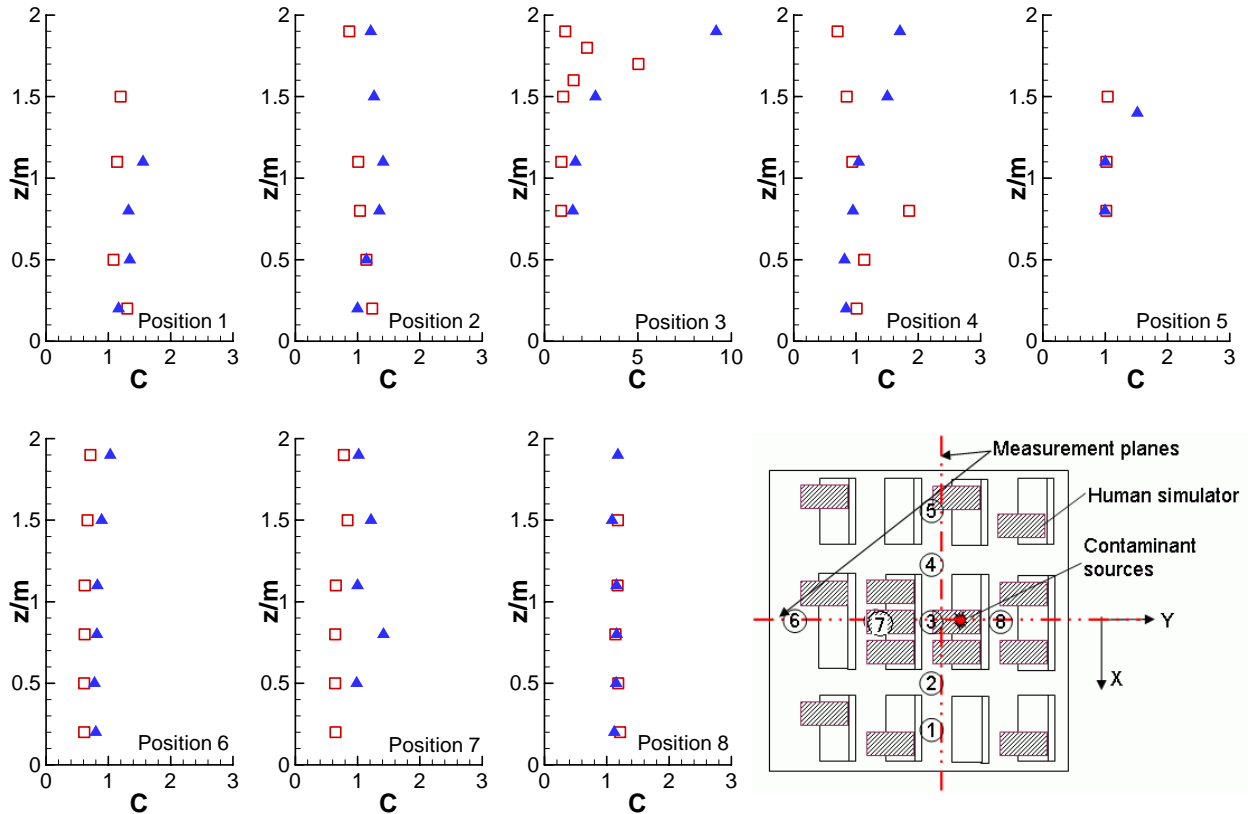

Fig. 8. Comparison of measured concentration distributions of the tracer gas (red rectangles) and the particulate matter (blue triangles) in different locations. The concentration was normalized in accord with Figures 6 and 7.

This study also shows that a cabin environment is similar to a building environment as they both are ventilated and enclosed spaces. Therefore, the integrated CFD tool presented in the paper for airflow and contaminant transportation modeling can be also applied to building environment upon appropriate validations [13-15].

6. Conclusions

This study investigated airflow and contaminant transport in an occupied cabin by both experimental measurements and numerical simulations with CFD. A four-row, twin-aisle mockup with 28 seats were built to measure the air velocity, air temperature, tracer gas and particle distributions. A half of the seats were occupied by heated human simulators, and an

14

environmental control system was used to simulate airflow pattern in the mockup. The numerical simulations used CFD with the RNG k-ε model and a Lagrangian particle trajectory model.

The simulated results were compared with the measured data. Due to the difficulties in measuring accurate flow boundary conditions from the air supply diffusers, the discrepancies are significant between the computed and measured airflow patterns. The predicted distributions of air temperature, tracer-gas concentration, and particulate concentration reasonably agree with the measured data, due to the complete mixing conditions in the cabin. This study also confirmed that both experiment and computations were not free from errors. A complete and accurate validation for the complex flow in a cabin is challenging and difficult.

The present study also analyzed the similarities and differences of transport and dispersion between the gaseous and particulate contaminants. The sub-micron-sized heavy particles behaved like the passive gas contaminant in the cabin except in the region near the source position because the diffusivity can be different.

Acknowledgements

References

[1] Olander L, Westlin A. Airflow in aircraft cabin, Staub – Reinhaltung der Luft 1991; 51(7-8): 283-288.
[2] Aboosaidi F, Warfield MJ, Choudhury D. Computational fluid dynamics applications in airplane cabin ventilation system design. Proceedings - Society of Automotive Engineers 1991; 246: 249-258.
[3] Mizuno T, Warfield MJ. Development of three-dimensional thermal airflow analysis computer program and verification test. ASHRAE Transactions 1992; 98(2): 329-338.
[4] Singh A, Hosni MH, Horstman, RH. Numerical simulation of airflow in an aircraft cabin section. ASHRAE Transactions 2002; 108(1): 1005-1013.
[5] Garner RP, Wong KL, Ericson SC, Baker AJ, Orzechowski JA. CFD validation for contaminant transport in aircraft cabin ventilation flow fields. Proceedings of Annual SAFE Symposium (Survival and Flight Equipment Association) 2003; p. 248-253.
[6] Lin CH, Wu TT, Horstman RH, Lebbin PA, Hosni MH, Jones BW, Beck BT. Comparison of large eddy simulation predictions with particle image velocimetry data for the airflow in a generic cabin model. Journal of HVAC&R Research 2005; 12 (3c): 935-951.

[7] Zhang Y, Sun Y, Wang A, Topmiller JL, Bennett JS. Experimental characterization of airflows in aircraft cabins, part II: results and research recommendations. ASHRAE Transactions 2005;111(2): 53-59.

[8] Mo H, Hosni MH, Jones BW. Application of particle image velocimetry for the measurement of the airflow characteristics in an aircraft cabin. ASHRAE Transactions 2003; 109(2):101-110.

[9] Yakhot V, Orszag SA. Renormalization group analysis of turbulence. Journal of Scientific Computing 1986; 1: 3-51.

[10] Chen Q. Comparison of different k-ε models for indoor air flow computations. Numerical Heat Transfer, Part B 1995; 28: 353-369.

[11] Zhang Z, Zhang W, Zhai JZ, Chen Q. Evaluation of various turbulence models in predicting airflow and turbulence in enclosed environments by CFD: Part-2: Comparison with experimental data from literature. HVAC&R Research 2007; 13(6): 871-886.

[12] Fluent. Fluent 6.2 Documentation. Fluent Inc., Lebanon, NH; 2005.

[13] Zhang Z, Chen Q. Experimental measurements and numerical simulations of particle transport and distribution in ventilated rooms. Atmospheric Environment 2006; 40(18): 3396-3408.

[14] Yuan X, Chen Q, Glicksman LR. Models for prediction of temperature difference and ventilation effectiveness with displacement ventilation. ASHRAE Transactions 1999; 105(1): 353-367.

[15] Zhang Z, Chen Q. Comparison of the Eulerian and Lagrangian methods for predicting particle transport in enclosed spaces. Atmospheric Environment 2007; 41: 5236-5248.

[16] Lai ACK, Chen FZ. Comparison of a new Eulerian model with a modified Lagrangian approach for particle distribution and deposition indoors. Atmospheric Environment 2007; 41: 5249-5256.

[17] Zhao B, Yang C, Yang X, Liu S. Particle dispersion and deposition in ventilated rooms: testing and evaluation of different Eulerian and Lagrangian models. Building and Environment 2007; 43(4): 388-397.

[18] Zhang T, Chen Q, Lin, CH. Optimal sensor placement for airborne contaminant detection in an aircraft cabin. HVAC&R Research 2007; 13(5): 683-696.

[19] Baker AJ. On validation for CFD prediction of mass transport in an aircraft passenger cabin. Private communication. University of Tennessee, Knoxville; 2005.